EVS30 Symposium
Stuttgart, Germany, October 9 - 11, 2017

Development of Integrated Power Control Algorithm for a Series-Parallel Type PHEV

Sungbae Jeon, Junbeom Wi, Yoonuk Kim, Jiho Yoo, Hyunsoo Kim

Hyunsoo Kim(corresponding author), School of Mechanical Engineering, Sungkyunkwan University, 2066, Seobu-ro, Jangan-gu, Suwon-si, Korea, hskim@me.skku.ac.kr

Summary

In this study, an integrated vehicle power control algorithm was developed for a series-parallel type PHEV to improve the fuel economy using the battery SOC rate and remaining time to the destination. To analyze the power characteristics, dynamic models of the target PHEV powertrain were obtained considering the mechanical loss. The backward simulator of the target PHEV was developed using dynamic programming. The backward simulations for various target SOC rate were performed to obtain the optimal mode shift map. The performance of the integrated control algorithm was evaluated for various routes and its fuel economy was compared with the existing CD-CS control.

Keywords: Plug-in hybrid electric vehicle, Integrated control, SOC rate, Dynamic programming

1 Introduction

PHEV(plug-in hybrid electric vehicle) can implement several driving modes depending on the design configuration using the engine and one or two MGs(motor-generator)[1]. The driving mode of PHEV includes EV(electric vehicle) mode, series mode, parallel mode and powersplit mode, etc. PHEV performance depends on not only the powertrain configuration but also its control strategy. The control strategy of PHEV consists of a vehicle power management strategy of and a battery energy management strategy. The power management control selects the driving mode and distributes the power according to the demanded wheel torque and vehicle speed. A CD-CS(charge depleting-charge sustaining) control has been generally used as a battery energy management strategy. In the CD control, the EV mode is mostly used and the battery SOC(state of charge) is reduced until it drops to the SOC limit. In the CS control, the engine is operated to sustain the SOC level[2]. When the CD-CS control is used, the engine sometimes has to be operated at low efficiency to sustain the battery SOC. In order to improve the fuel economy of PHEV, it is necessary to manage the battery SOC by proper control of the engine operation. In addition, since the battery capacity of PHEV is about four times larger than that of HEV(hybrid electric vehicle), the control strategy for the CD range has significant influence on the fuel economy[3].

Since the PHEV has multiple power sources, various driving mode can be operated for the same driving condition. When the vehicle speed profile is known in advance, the global optimization method, DP(dynamic programming) can be used. Using DP, many studies were performed to select the most efficient driving mode[4]. The optimal SOC trajectory to minimize the fuel consumption while satisfying the final SOC can be found from DP. DP can be used primarily as a tool to find the fuel economy potential, rather than an actual hybrid vehicle controller. Finding the optimal SOC trajectory should be fully aware of the speed profile and requires a large amount of computation time, which makes it difficult to apply in the real driving environment[5]. Therefore, it is necessary to develop a novel control algorithm which can be applied in real time to improve the fuel economy of the PHEV.

In this study, an integrated battery energy-vehicle power control algorithm was proposed for a series-parallel type PHEV. First, forward simulator of the target PHEV was developed to implement the driving modes. To obtain the global optimal SOC trajectory, the backward simulator for the target PHEV was developed using dynamic programming. Using the remaining time to the destination and battery SOC information, the integrated battery energy-vehicle power control algorithm was developed. Finally, the integrated battery energy-vehicle power control algorithm was evaluated by comparing the existing CD-CS control for various driving cycle.

2 Development of Series-Parallel Type PHEV Forward Simulator

2.1 Structure of the target PHEV

Figure1 represents the schematic diagram of the series-parallel type PHEV investigated in this study. The target PHEV is composed of the engine, MG(motor generator)1, MG2, clutch, battery, and several gears. In this configuration, the engine can be operated independent of the vehicle speed when the clutch is disengaged, which functions as a series type. When the clutch is engaged, the engine operates with MG2 which plays like a parallel type.

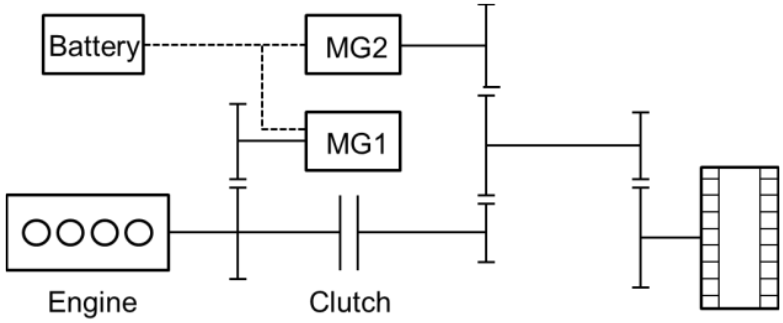

Figure1 Structure of series-parallel type PHEV

2.2 Powertrain model

To develop the forward simulator, the powertrain model of target PHEV was obtained.

Engine: The engine was modeled using the characteristic map as shown in Figure2a. The engine dynamics was expressed as follows:

$$J_{eng} \cdot \dot{\omega}_{eng} = T_{eng} - T_{eng\_loss} \quad (1)$$

where J is the rotational inertia, ω is the rotational speed and T is the torque. The subscript eng denotes the engine and eng_loss denotes the engine loss.

Motor/generator: MG1 and MG2 were modeled using the characteristic map as shown in Figure2b and 2c. The MGs power can be expressed as follows:

$$P_{MG} = \frac{T_{MG} \cdot \omega_{MG}}{\eta_{MG}} \quad (2)$$

$$P_{MG} = T_{MG} \cdot \omega_{MG} \cdot \eta_{MG} \quad (3)$$

where P is the power and η is the efficiency which is a function of the MG torque and MG rotational speed, the subscript MG represents the motor-generator.

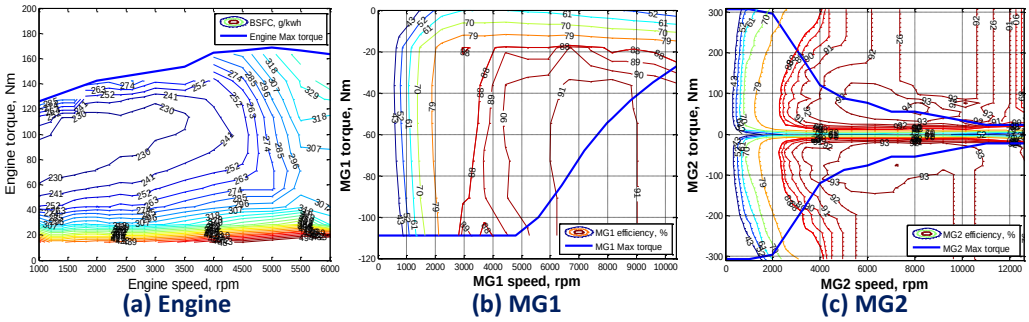

Figure2 Characteristic maps of the engine(a), MG1(b) and MG2(c)

Clutch: The clutch engagement and disengagement is determined by the pressure acting on the clutch. The clutch torque is expressed as follows:

$$T_{cl} = \mu_{cl} \cdot N_{cl} \cdot A_{cl} \cdot \frac{2(r_o^3 - r_i^3)}{3(r_o^2 - r_i^2)} \cdot p(t) \tag{4}$$

where μ is the friction coefficient, N is the number of surfaces, A is the area, r is the radius and p is the pressure acting on the clutch. The subscript *cl* denotes the clutch, *o* is the outer value and *i* is the inner value.

Battery: The electrical energy of the battery is represented by the SOC(state of charge). SOC can be expressed by the following equation using the current integration method[6],

$$SOC = SOC_{init} - \frac{1}{C_{bat}} \int_{t_{init}}^{t} \frac{P_{bat}}{V_{bat}} dt \tag{5}$$

where C is the capacity, t is the time and V is the voltage. The subscript *init* denotes the initial value and *bat* denotes the battery.

Vehicle: The vehicle longitudinal dynamics is represented as,

$$M \cdot \dot{v} = F_{tra} - F_{road} \tag{6}$$

where M is the vehicle mass, v is the vehicle speed and F is the force. The subscript tra denotes the traction and road denotes the road load

23 Component loss model

To investigate the powertrain characteristics in detail, powertrain loss needs to be included. In this study, the gear loss, the clutch loss and MG1 unloaded loss were considered.

Gear loss: The gear torque loss was assumed to be 1% of the transmitted torque, which is expressed as follows[7]:

$$T_{gear\_loss} = T_{in} \cdot (1 - \eta_{gear}) \cdot sign(P_{in}) \tag{7}$$

where the subscript *in* denotes input. And sign term represents the sign of the gear loss depending on the direction of power.

Clutch loss: The clutch loss occurs due to the relative movement of friction surfaces in the form of the shear force, which generates a drag torque. The drag torque in clutch can be expressed follows[8]:

$$T_{cl\_loss} = 2 \cdot \pi \cdot N_{cl} \int_{r_i}^{r_o} \alpha \frac{\mu r^3}{h} \omega_{rel} C_f dr \tag{8}$$

where α is the film formation rate, *h* is the clearance and *C* is the turbulent shear stress factor. The subscript *cl_loss* denotes the clutch loss, *f* denotes the friction, and *rel* denotes relative value.

MG1 unloaded loss model: When MG does not generate torque and rotates freely only by the external force, MG unloaded loss occurs according to the rotational speed. In parallel mode of the target PHEV, the MG1 unloaded loss occurs since the clutch is engaged. In this study, the MG1 unloaded loss was modeled using experimental data.

2.4 Driving modes

The target PHEV is driven in four modes: EV mode, series mode, parallel mode. In the EV mode, MG2 supplies all the required vehicle power using the battery energy. Figure3a shows the power flow in the EV mode. In the EV mode, the battery power considering the efficiency of battery and MG2 is expressed as follows:

$$P_{bat} = \frac{P_{MG2}}{\eta_{MG2} \cdot \eta_{bat}} \tag{9}$$

where P is the power, η is the efficiency. And the subscript bat denotes the battery, MG2 denotes the second motor generator.

In the series mode, the clutch is disengaged and MG2 supplies all the required vehicle power in the same way as the EV mode, but MG1 generates and charges the battery using the engine power. Figure3b shows the power flow in the series mode. The battery power for the MG2 propulsion and MG1 power generation is expressed as follows:

$$P_{bat} = P_{MG1} \cdot \eta_{MG1} \cdot \eta_{bat} + \frac{P_{MG2}}{\eta_{MG2} \cdot \eta_{bat}} \tag{10}$$

In the parallel mode, the clutch is engaged and the engine speed is dependent on the vehicle speed. Figure3c shows the power flow of the parallel mode. The engine power is transmitted to the vehicle directly and MG2 is motoring or generating according to the engine operating point. Because the EV mode and series mode cannot operate over the MG2 maximum power, the parallel mode is used when the wheel power is larger than the MG2 maximum power. The battery power in parallel mode considering the MG2 generating or motoring can be expressed as follows:

$$P_{bat} = \frac{P_{MG2}}{\eta_{MG2} \cdot \eta_{bat}} \quad \text{(MG2 motoring)} \tag{11}$$

$$P_{bat} = P_{MG2} \cdot \eta_{MG2} \cdot \eta_{bat} \quad \text{(MG2 generating)} \tag{12}$$

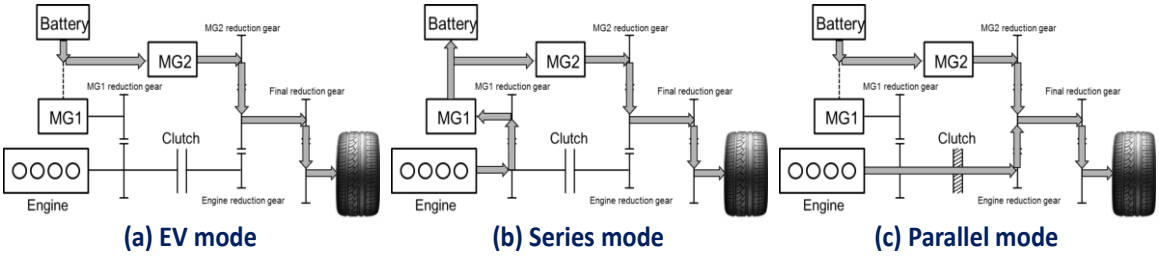

Figure3 Driving modes of the target PHEV

3 Development of Series-Parallel Type PHEV Backward Simulator

3.1 Local optimization

To develop the target PHEV backward simulator, dynamic programming(DP), which is a global optimization method was used. In this study, DP is used to solve the optimization problem to select the driving mode and determine the operating points of the engine and MGs which minimize the fuel consumption when the driving cycle is given. The fuel rate determined from the engine operating point and BSFC map (Figure2a) is expressed as follows[9]:

$$\dot{m}_{fuel} = L(T_{eng}, \omega_{eng}) \tag{13}$$

where ṁ is the mass rate. The subscript fuel denotes the fuel consumption.

A local optimization is a process to obtain the minimum fuel consumption according to the battery power. To obtain the minimum fuel consumption, the engine and MGs operating points should be expressed as functions of battery power.

In the series mode, the engine speed and MG1 speed are independent of the wheel speed. The MG1 operating point is determined by the engine operating point as follows:

$$T_{MG1} = -\frac{T_{eng}}{N_{MG1}} \cdot \eta_{gear} \tag{14}$$

$$\omega_{MG1} = \omega_{eng} \cdot N_{MG1} \tag{15}$$

where N is the gear ratio. The MG1 operating point is a function of the engine operating point, and the MG2 operating point is determined by the vehicle speed and wheel torque. So the battery power in the series mode(Eq. 10) becomes a function of the engine operating point (T_{eng},ω_{eng}), which is expressed as,

$$P_{bat} = f(T_{MG1}, \omega_{MG1}, T_{MG2}, \omega_{MG2}) = f(T_{eng}, \omega_{eng}) \tag{16}$$

As shown in Eqs. (13), (16), both the fuel rate and battery power are functions of the engine operating point. To perform the local optimization, the engine operating point having the smallest fuel rate was selected among various engine operating points with the same battery power. The fuel rate of local optimized operating point can be represented only a function of the battery power as follows[10]:

$$\dot{m}_{fuel} = L\left({T_{eng}}^*, {\omega_{eng}}^*\right) = g(P_{bat}) \tag{17}$$

where the superscript * denotes the local optimized value.

In the parallel mode, the clutch is engaged and the engine speed is dependent of the vehicle speed. The engine and MG2 supply the required vehicle power, and MG1 is free rotating. When the engine operating point is determined, the MG2 operating point is also determined to satisfy the required vehicle power. The battery power in parallel mode is expressed as follows:

$$P_{bat} = f(T_{MG2}, \omega_{MG2}) = f(T_{eng}, \omega_{eng}) \tag{18}$$

Since both the battery power and fuel rate in parallel mode are also functions of the engine operating point, the fuel rate in parallel mode becomes a function of the battery power.

3.2 Global optimization

After the fuel rate was determined as a function of the battery power through the local optimization, a global optimization was performed to minimize the fuel consumption. Since the fuel rate is the function of the battery power and driving mode, control variables are the battery power and driving mode. And state variable is the battery power. The global optimization problem is represented as follows[10]:

$$Minimize\ h(x_{k=1}) + \sum_{k=2}^{N} g_{k-1}(P_{bat}(k-1), Mode(k-1)) \tag{19}$$

$$subject\ to\ \Delta SOC(k-1) = f\left(P_{bat}(k-1), Mode(k-1)\right) \tag{20}$$

where x is the state variable, k is the step time, N is the driving cycle final time step, Mode is the operating mode.

A cost function of the global optimization problem is expressed as follows:

$$min \quad {J_k}^*(x_k) = g_{k-1}(P_{bat}(k-1), Mode) + {J_{k-1}}^*(x_{k-1}) \tag{21}$$

where J_k^* is the optimal fuel consumption from the first step to k step.

3.3 Backward simulator for the target PHEV

The backward simulation process is as follows: first, driving cycle, initial and final SOC are selected. To calculate the local optimal fuel rate, MG1, MG2 and engine operating points of each mode, the local optimization process is carried out for the wheel speed and torque at each step. The backward simulation is finished by obtaining the fuel consumption field and finding optimal trajectory.

4 Integrated Battery Energy-Vehicle Power Control Algorithm

In the existing CD-CS control, when the battery SOC is sufficient, the vehicle is driven mostly in the EV mode. When the battery SOC is lower than the lower limit, the CD-CS control selects a driving mode that uses the engine to sustain the battery SOC. In this case, a driving mode which has lower efficiency could be selected instead of the driving mode with higher efficiency.

To solve this problem, an integrated battery energy-vehicle power control algorithm was proposed, which manages the battery SOC in advance. First, the difference between the present SOC and the final SOC is divided by the remaining time to the destination. The remaining time to the destination can be obtained from the navigation. Next, the target SOC rate was defined as follows:

$$\dot{SOC}_{target} = \frac{SOC - SOC_{final}}{\Delta t_{dest}} \tag{22}$$

where the subscript target denotes the target value, and dest means the destination.

When the target SOC rate is determined, it is necessary to get an optimal mode shift map for each target SOC rate. To obtain the optimal mode shift map, backward simulations for various target SOC rates were performed.

Figure4 shows the SOC trajectories by the backward simulations for the target SOC rate range 0/h to 0.5/h. When the target SOC rate is 0/h, the initial SOC is the same with the final SOC, which implies the CS mode.

For UDDS cycle, it is seen from Figure4a that the overall charging and discharging trend are similar. However, in high speed range 200 ~ 310sec(region A), battery charging and discharging rate showed different behavior depending on the target SOC rate. When the target SOC rate was 0/h ~ 0.3/h, the battery was charged in region A. On the other hand, when the target SOC rate was 0.4/h ~ 0.5/h, the battery was discharged the electric energy. In region A, the parallel mode can used because the engine speed is over the engine idle speed. When the parallel mode is used, the battery can be charged or discharged depending on the power distribution of the engine and MG2.

For HWFET cycle(Figure4b), the parallel mode was used in most region. The SOC trajectory showed similar fashion for all SOC rate. In region B and C(265 ~ 295sec, 715 ~765sec), the SOC increased due to regenerative braking.

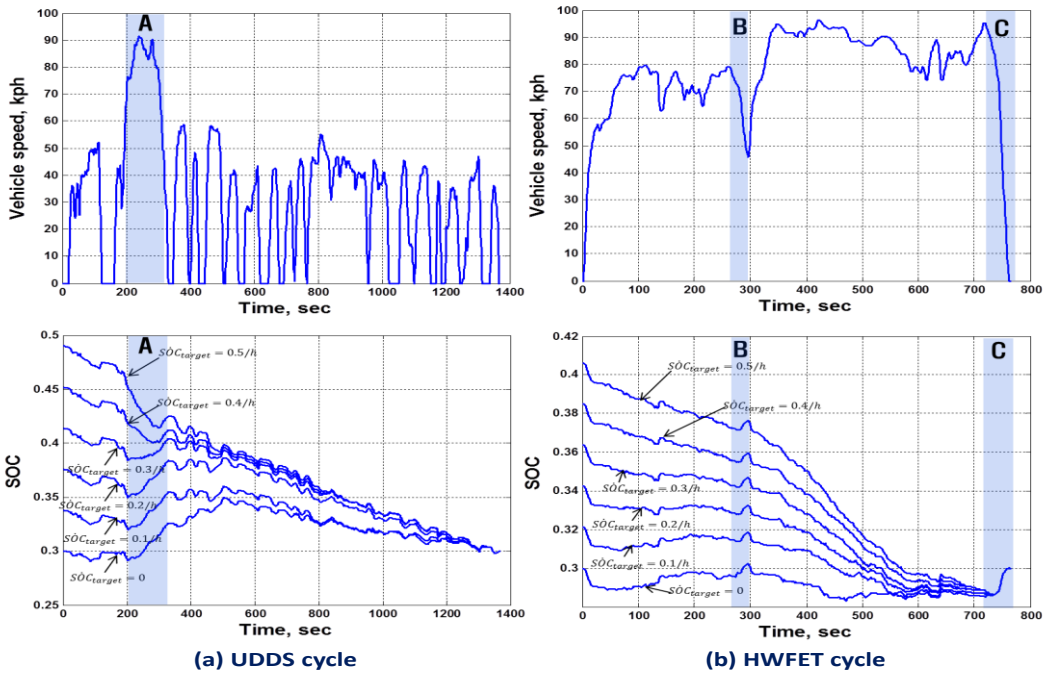

Figure4 SOC trajectories for various $\dot{SOC}_{target}$

Figure5 shows driving mode with respect to the demanded wheel torque and vehicle speed for various target SOC rate. As the target SOC rate increased, the area of EV mode increased gradually. The series mode was mainly used under 48km/h region. When the target SOC rate is larger than 0.3/h, series mode was seldom used. The parallel mode was only used over 48km/h region. As the target SOC rate increased, the area of parallel mode decreased gradually.

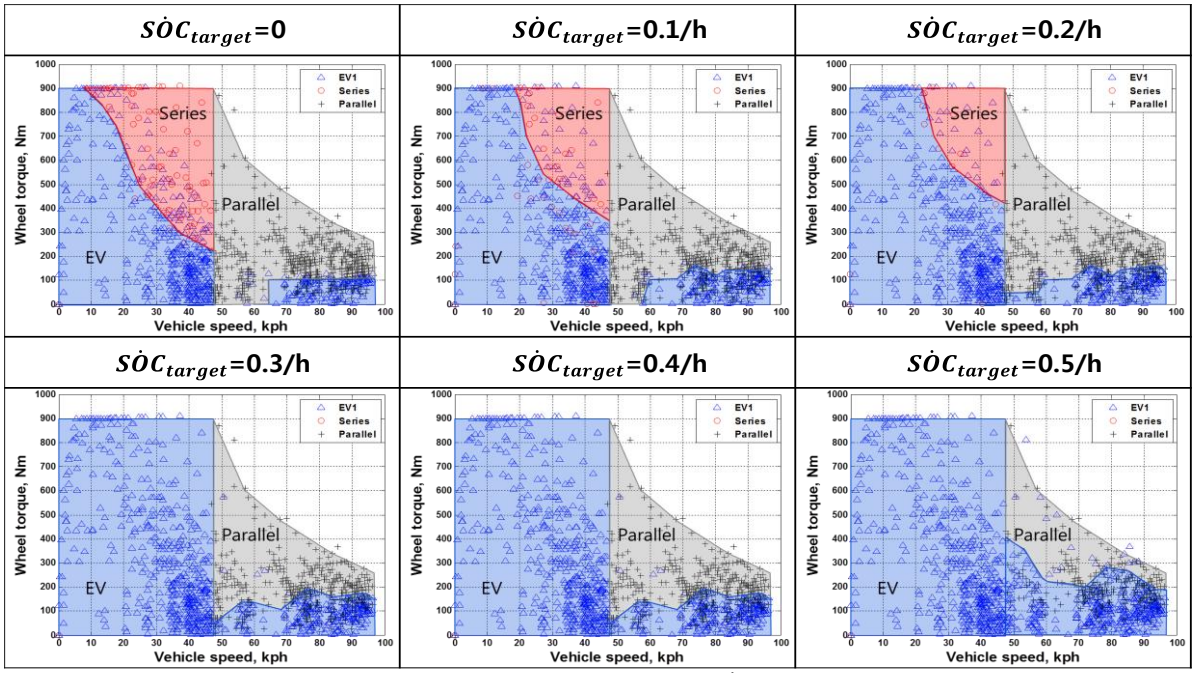

Figure5 Mode shift map for various $\dot{SOC}_{target}$

Using the target SOC value, the driving mode was selected from the mode shift map which was obtained for various target SOC rate in Figure5. Using the selected mode shift map, the driving mode was determined according to the demanded wheel torque and vehicle speed. When mode shifting, the torque and time hysteresis were considered to prevent the frequent mode shift. Figure6 shows the proposed integrated control algorithm.

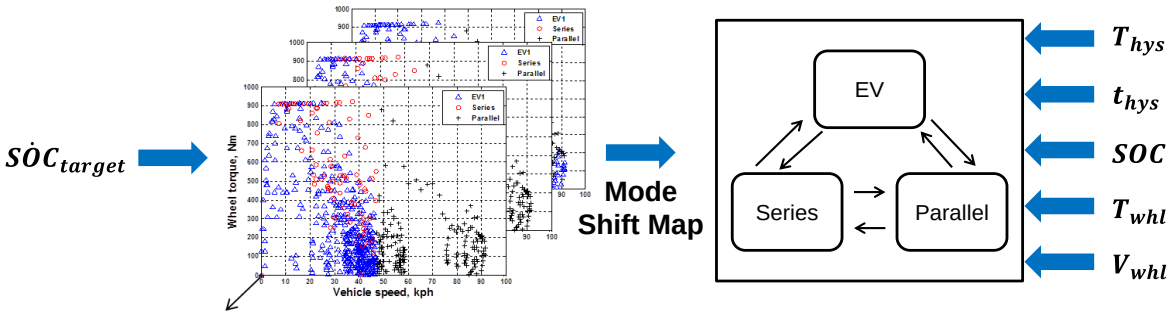

Figure6 Integrated battery energy-vehicle power control algorithm

5 Performance of the integrated control

To evaluate the performance of the integrated control algorithm, simulations were performed for real road cycle SKKU#1 route and SKKU#2 route which consist of the city, highway driving and slope. In this comparion, the mode shift maps obtained by backward simulation for UDDS and HWFET cycle were used.

Figure7a shows SKKU#1 route, which is 10.73km distance. Considering the travel distance, the initial SOC was set 40% to compare with the CD-CS control. The real load cycle has an elevation though the route and the effect of the elevation was included in the demanded wheel torque. Figure7b shows

SKKU#2 route, which is 25.00km distance. Since the distance of SKKU#2 route is longer than that of SKKU#1, the initial SOC was set 60%.

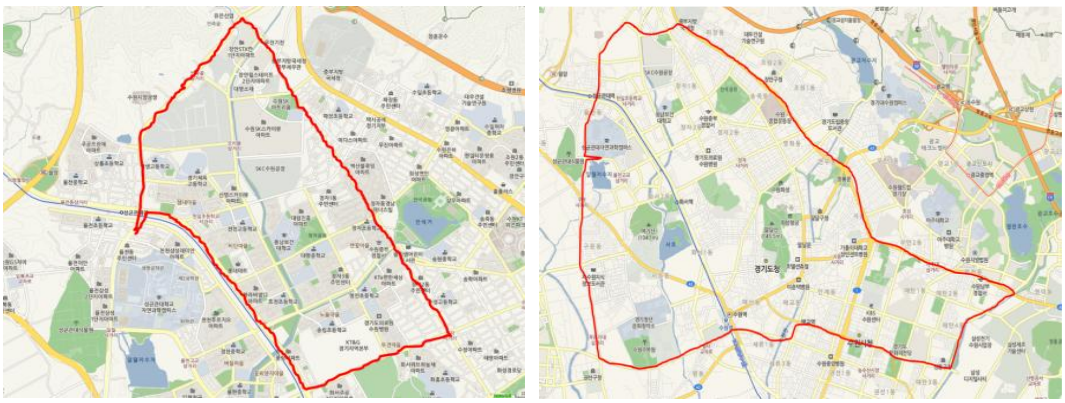

(a) SKKU#1 route **(b) SKKU#2 route**

Figure7 Real road cycle SKKU#1 and SKKU#2 route

Figure8a shows the simulation results for SKKU#1 route. In the CD-CS control, only the EV mode was used until the battery SOC was reduced to 30% at t=482sec(point P). After the point P, the series and parallel mode were used to maintain the battery SOC close to 30%(b). The fuel consumption of the CD-CS control was zero until the point P. After that point, the fuel consumption increased rapidly since the series and parallel mode were used to sustain the battery SOC(d).

On the other hand, the integrated control used the series and parallel mode according to the driving condition and target SOC rate value. In the acceleration region A(t=0 ~ 264sec), the integrated control consumed the battery energy to 39.6%(c) using the series and parallel in advance while the fuel was used by 129.5g(d). In the last region B(869 ~ 1181sec), the integrated control only used the EV mode(b). Since the battery SOC was sufficient, the engine was not operated in this region.

Figure8b shows the simulation results for SKKU#2 route. In the CD-CS control, only the EV mode was used until the battery SOC was reduced to 30% at t=1895sec(point Q). After the point Q, the CD-CS control began to use the parallel and series mode to sustain the battery SOC(b). The CD-CS control never used the fuel before the point Q. After the point Q, the fuel consumption increased rapidly using the series and parallel mode(d). On the other hand, in the integrated control, the battery SOC decreased linearly to 30% throughout the entire route(c). The fuel consumption increased whenever the engine was operated(d).

Table1 shows the comparison of the integrated control and CD-CS control for SKKU#1 and SKKU#2 route. When driving SKKU#1 route, the integrated control consumed the fuel 212.5g which was less than that of the CD-CS control 217.2g. The final SOC of integrated control was 30.96% which was larger than that of the CD-CS control 30.48%. Accordingly, the equivalent fuel economies of the integrated control and CD-CS control were 22.73km/l and 21.98km/l respectively. The equivalent fuel economy improvement of the integrated control was 3.4% compared to the CD-CS control.

When driving SKKU#2 route, the integrated control consumed less fuel than that of the CD-CS control. The final SOC of integrated control was 31.80% which was higher than that of the CD-CS control 30.69%. Accordingly, the equivalent fuel economies of the integrated control and CD-CS control were 24.70km/l and 23.54km/l, respectively. The equivalent fuel economy improvement of the integrated control was 4.7% compared to the CD-CS control.

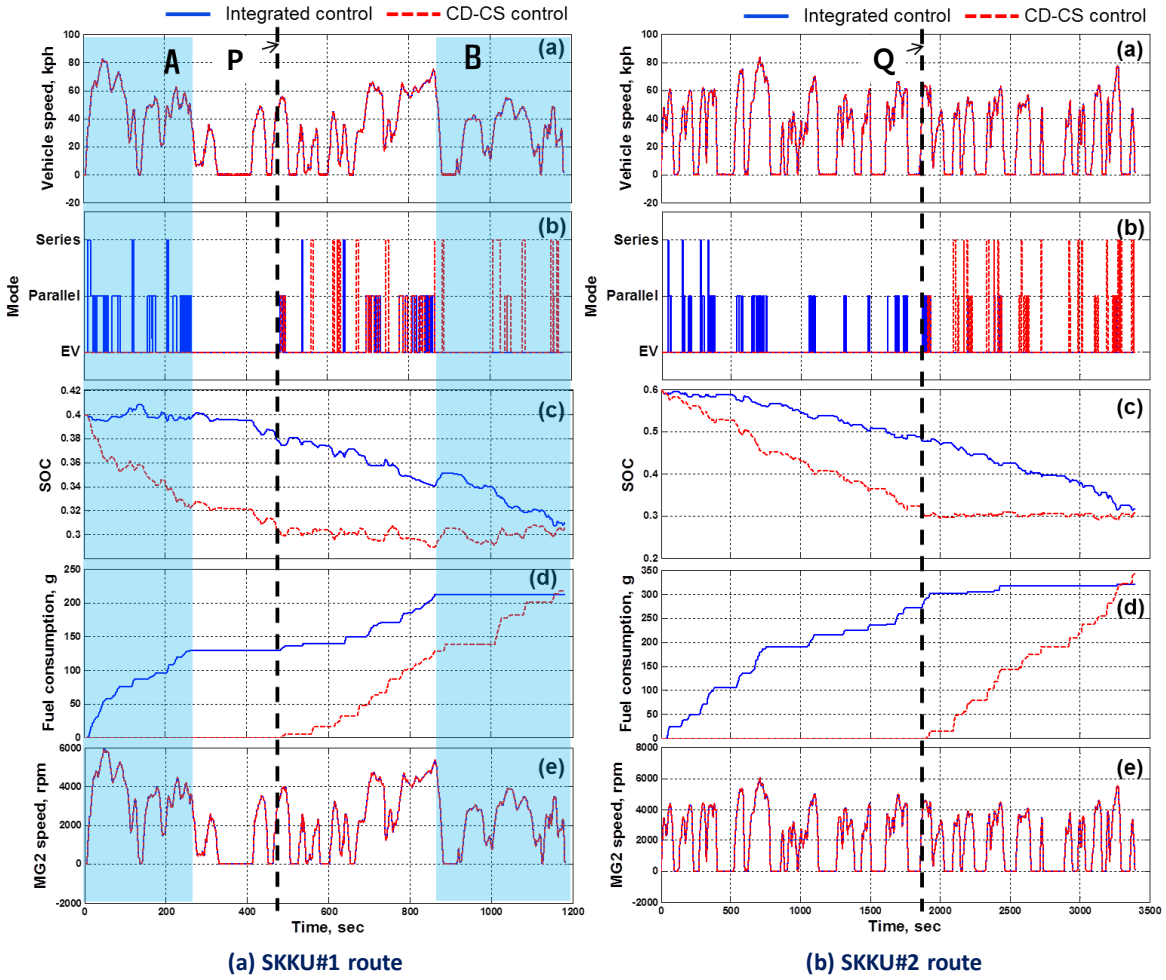

Figure8 Comparison of integrated control with CD-CS control for SKKU#1 and SKKU#2 route

Table1 Comparison of integrated control with CD-CS control for SKKU#1 and SKKU#2 route

Cycle		Fuel consumption(g)	Final SOC(%)	Equivalent fuel economy(km/l)	Improvement rate(%)
SKKU#1	CD-CS	217.2	30.48	21.98	-
	Integrated	212.5	30.96	22.73	+3.4
SKKU#2	CD-CS	341.9	30.69	23.54	-
	Integrated	321.6	31.80	24.70	+4.7

As shown in the simulation results in Table1, it was found that the equivalent fuel economy by the integrated control can be improved compared to the existing CD-CS control. Since the integrated control only requires the present battery SOC and the remaining time to the destination, it can be implemented in real time environment. For example, when the remaining time was suddenly increased due to the heavy traffic, the target SOC rate was updated in real time using the updated remaining time and the present battery SOC information.

6 Conclusions

In this study, an integrated battery energy-vehicle power control algorithm was developed for a series-parallel type PHEV to improve the fuel economy.

First, the forward simulator of the target PHEV which consists of the engine, MGs, clutch, battery and vehicle was developed. To investigate the powertrain characteristics, the gear loss, clutch loss and MG1 unloaded loss were considered. The driving modes of the target PHEV which consist of the EV mode, series mode, parallel mode were analyzed. Next, the backward simulator of the target PHEV was developed using the dynamic programming. The local optimization was used to obtain the minimum fuel consumption according to the battery power. The global optimization was performed to minimize the fuel consumption. Based on the local and global optimization, the optimal trajectory which guarantees the minimum cumulative fuel consumption was obtained.

The integrated battery energy-vehicle power control algorithm was developed using the remaining time to the destination and SOC information. The backward simulations for various target SOC rate were performed for UDDS and HWFET cycle to obtain the optimal mode shift map.

The performance of the integrated control algorithm was evaluated by comparing with the existing CD-CS control. simulations were performed for SKKU#1 route(10.73km) and SKKU#2 route(25.00km) which consist of the city, highway driving and slope. It was found that the equivalent fuel economy by the integrated control was improved by 3.4%(SKKU#1) and 4.7%(SKKU#2), respectively compared to the CD-CS control.

References

[1] K. Ahn and P.Y. Papalambros, *Engine optimal operation lines for power-split hybrid electric vehicles*, Journal of Automobile engineering, Vol. 223 (9), 2009, 1149-1162

[2] H.C. Watson and S. Alihikari, *Performance Comparison of Engine Down-Sized to High Efficiency ICEs in Optimized Hybrid Vehicles*, SAE paper No. 2012-01-1033, 2012

[3] J. Jeong et. Al., Analysis of Fuel Economy and Battery Life depending on the Types of HEV using Dynamic Programming, IEEE 2013 World Electric Vehicle Symposium and Exhibition (EVS27), 2013, 1-5

[4] T. Leroy and J. Malaise, *Towards real-time optimal energy management of hev powertrains using stochastic dynamic programming*, IEEE Vehicle Power and Propulsion Conference, Seoul, Korea, Oct 9-12, 2012

[5] H. Banvait et. Al., *A Rule-Based Energy Management Strategy for Plug-in Hybrid Electric Vehicle (PHEV)*, IEEE American Control Conference, Saint Louis, Missouri, Jun 10-12, 2009

[6] Y. Yuan et. Al., *An improved hydrodynamic model for open wet transmission clutches*, Journal of Fluids Engineering, Vol. 123 (3), 2007, 333-337

[7] H. Shin et. Al., *Development of an Integrated Energy Management Strategy with Cabin Heating for Plug-in Hybrid Electric Vehicle*, the 10th International Conference on Ecological Vehicles and Renewable Energies, Monte-Carlo, Monaco, Mar 31-Apr 2, 2015

[8] J. Kang et. Al., *Comparative Analysis of Transmission Efficiency for One Mode and Two Mode Power Split Transmission*, The Spring Korean Society of Automotive Engineers Annual Conference, Busan, Korea, May 6-7, 2010

[9] J. Liu and H. Peng, *Modeling and Control of a Power-Split Hybrid Vehicle*, IEEE Control Systems Technology, Vol. 16 (6), 2008, 1242-1251

[10] C.C. Lin et. Al., *A stochastic control strategy for hybrid electric vehicles*, IEEE American Control Conference, Boston, Massachusetts, Jun 30-Jul 2, 2004

Authors

Sungbae Jeon
He received B.S. and M.S. in mechanical engineering from Sungkyunkwan University, Suwon, Korea, in 2015 and 2017. Currently, he is working at eco-vehicle research center of Hyundai Motor Company. His research interests include modeling and control of powertrain system for PHEV.

Junbeom Wi
He received B.S. in mechanical engineering from Sungkyunkwan University, Suwon, Korea, in 2016 where he has been working toward M.S. degree. His research interests include modeling and control of powertrain and hydraulic system for PHEV.

Yoonuk Kim
He received B.S. in mechanical engineering from Sungkyunkwan University, Suwon, Korea, in 2016 where he has been working toward M.S. degree. His research interests include modeling and control of powertrain and motor thermal management with cooling system for PHEV.

Jiho Yoo
He received B.S. in mechanical engineering from Sungkyunkwan University, Suwon, Korea, in 2016 where he has been working toward M.S. degree. His research interests include integrated braking system control.

Hyunsoo Kim
He received a B.S. in mechanical engineering from Seoul National University, Seoul, Korea, in 1977, a M.S. degree in mechanical engineering from the Korea Advanced Institute of Science and Technology, Seoul, Korea, in 1979, and a Ph.D. degree in mechanical engineering from the University of Texas at Austin, Texas, USA, in 1986.
Since 1986, he has worked as a Professor, Chairman, Dean of the College of Engineering and Executive Vice President at Sungkyunkwan University. His main research interests include drivetrain design of HEV and PHEV. He has authored numerous journal papers and patents.
Prof. Kim served as a President of Electric Drive Vehicle Division of the Korea Society of Automotive Engineers from 2005 to 2012 and presently serves on the editorial board of the International Journal of Automotive Technology and International Journal of Automobile Engineering.